Time Synchronization in IoT networks : case of a wireless body area network

Imen Nasr, Leila Najjar Atallah, Sofiane Cherif, Benoit Geller

Time synchronization in IoT Networks: Case of a Wireless Body Area Network

Imen Nasr [1,2], Leïla Najjar Atallah [1], Sofiane Cherif [1] and Benoît Geller [2]

[1] *University of Carthage, Higher School of Communications of Tunis (SUP'COM), Research Lab. COSIM*

[2] *Ecole Nationale Supérieure de Techniques Avancées ENSTA ParisTech, UPSA, France*

[1] {nasr.imen,leila.najjar,sofiane.cherif}@supcom.rnu.tn

[2] {imen.nasr,benoit.geller}@ensta-paristech.fr

***Abstract*— * In this paper, we propose a time synchronization algorithm for the WBAN frame structure specified by the IEEE 802.15.6 standard. This algorithm is based on a non coherent timing error detector under a Rayleigh fading channel. With the use of a such detector, the system complexity is reduced by getting rid of the phase recovery block. Simulation results show an enhancement in the system performance in terms of mean square errors (MSE) with respect to Non Data Aided (NDA) techniques.**

***Index Terms*—Time synchronization, ML estimation, WBAN, non-coherent detector.**

I. Introduction

In the future, billions of objects, machines and infrastructures will be globally connected. A huge volume of data and services are going to be processed into a worldwide network called the Internet of Things (IoT). The diversity of services in the IoT implies that enterprizes work together in order to offer complementary and interoperable services and to develop complete solutions [1]. An open platform is, therefore, essential to promote these partnerships.

IoT should cover the everyday human life. Thus, there is no limit for the distances between connected things. The role of an object is to transfer information gathered by a set of sensors to be treated by a distant processing unit and generate some tasks. As any emergent market, a transition period is required before the optimization of the whole system.

IoT can be used in different fields such as medical, sport, telecommunications, commercial, industrial and security domains. Two standards have already been defined for that purpose; IEEE 802.15.4 for Wireless Personal Area Networks (WPAN) and IEEE 802.15.6 for Wireless Body Area Networks (WBAN). In this paper, we are going to focus on the WBAN standard. It consists in a wearable network made by low-power-consumption emerging wireless technologies such as narrowband (NB) systems [2].

A WBAN is operating with different wireless technologies in the same frequency band. Time synchronization is therefore a mandatory task at the receiver, as it is processed at front-end, in order to insure reliable data transmission. Timing recovery enhances the robustness to noise, interference and contention. Low complexity synchronization algorithms are required in a WBAN to guarantee a low latency network and to extend the network lifetime as well.

In real systems, we usually implement either a Data Aided (DA) or a NDA time delay estimation techniques [3], [4]. Although DA techniques outperform NDA ones, they decrease the spectral efficiency and increase power consumption by the insertion of pilot signals. NDA time recovery techniques can be used to deal with this problem. This is obtained at the price of performance degradation in particular for low Signal to Noise Ratio (SNR). Some Code Aided (CA) techniques [5]–[7] have been proposed to boost the synchronizer performance by using soft information from the decoded signal at the timing recovery process. However, this technique is not preferable for a WBAN due to its implementation complexity [8]. A complexity reduced technique has been proposed in [9] for BPSK signals and in [10] for a WBAN framework under an AWGN channel. It consists in introducing of the soft demapper output into the synchronizer to enhance the time delay estimation with no need for pilot signals. In this paper, we are going to present a low complexity time synchronization algorithm for a non coherent receiver under a Rayleigh flat fading channel. This algorithm is suitable for DPSK modulated signals specified by the IEEE 802.15.6 standards for a NB WBAN and allows to get rid of the carrier phase recovery process.

This paper is organized as follows. In section II, we present the WBAN standard specifications for the NB systems which operate in the 2.4GHz frequency band. In section III, a time synchronization algorithm for a non coherent receiver under a complex gaussian fading channel is proposed. Simulation results are given in section IV to evaluate our proposed algorithm. Some conclusions are provided in the last section.

In what follows, $\Re\{x\}$ stands for the real part of x and $\Im\{x\}$ for the imaginary part of x. x^* is the conjugate of x. $\otimes$ is the convolution operator and for any function f, f' is its first derivative.

II. WBAN Standard specification

WBAN is a network of wireless sensors placed on and/or into the body. These sensors are used for e-Health applications, this is why, they require particular standard specifications especially in terms of power usage. The IEEE 802.15.6 working

*This work has been supported by the Greencocom project of the ANR program

group has already defined the physical (PHY) and medium access control (MAC) layers specifications. The MAC layer is responsible of choosing channel access, packet scheduling and signaling techniques in order insure an efficient power budget management. The PHY layer is responsible of the frequency selection, the carrier frequency generation, signal detection including timing recovery, modulation/demodulation process and information encryption and decryption.

Energy consumption at the PHY layer can be affected by the environment of application, the modulation and the frequency bandwidth choice. DPSK modulation was specified by the standard since it is a low range mapping technique that requires low throughput and thus low energy. Furthermore, by selecting a differential modulation, a non coherent signal detection technique can be implemented at the receiver. This type of receiver does not need the phase information of the transmitter carrier to recover the signal. Thus, it does not require expensive and complex carrier recovery circuits. It however leads to higher bit error rate with respect to a coherent receiver [11].

Depending on the radio spectrum regulation constraints of the countries all over the world, different frequency bandwidth options were proposed by the standard. Based on the selected frequency range, three sub-layers are proposed for the PHY: the NB, the Ultra Wideband (UWB) and the Human Body Communications (HBC). In this paper, we are interested in the NB sub-layer dedicated to the communication of sensors implemented into or placed on the body. In TABLE I, we summarize the coding and modulation specifications of the standard for NB-WBAN operating in the frequency range $[2400\text{MHz}, 2483.5\text{MHz}]$. The system uses

Packet Component	Modulation	Symbol Rate (kbps)	Code Rate (k/n)	Spreading Factor	Data Rate (kbps)
PLCP Header	$\frac{\pi}{2}$-DBPSK	600	19/31	4	91.9
PSDU	$\frac{\pi}{2}$-DBPSK	600	51/63	4	121.4
PSDU	$\frac{\pi}{2}$-DBPSK	600	51/63	2	242.9
PSDU	$\frac{\pi}{2}$-DBPSK	600	51/63	1	485.7
PSDU	$\frac{\pi}{4}$-DQPSK	600	51/63	1	971.4

TABLE I: Modulation and Coding Specifications

a systematic BCH$(63, 51, t = 2)$ or a shortened systematic BCH$(31, 19, t = 2)$ encoder where $t = 2$ is the number of errors the decoder is able to correct. The BCH code is known for its low decoding complexity. The limited number of redundant bits does not lead to a huge increase in the power consumption.
In order to obtain a constant symbol rate, a spreading factor that depends on the modulation, the coding and the data rate. At low SNR, we opt for a low order modulation.

The main issue of the logical layer is to provide a method for transforming a physical-layer service data unit (PSDU) into a physical-layer protocol data unit (PPDU). As shown in Fig. 1, during the transmission, the PSDU is preceded by a preamble and a header to form the PPDU. The last two components serve as aids in the PSDU demodulation and delivery.

The same figure presents the format of the PPDU composed of the Physical Layer Convergence Protocol (PLCP) preamble, the PLCP header and the PSDU. The PLCP preamble is is constructed by the concatenation a 63-bit-length m-sequence u with a specific 27-bit-length extension sequence [1]. The preamble length is thus equal to 90 bits. The preamble is used by the receiver during the timing recovery process.

The PLCP header is the second main component of the PPDU. This component conveys the necessary information about the PHY parameters to help the receiver to decode the PSDU. The size of the PLCP header is equal to 31 bits.

The last component of the PPDU is the PSDU. It contains the useful transmitted data.

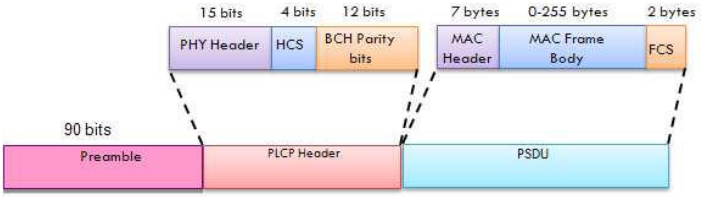

Fig. 1: Standard PPDU structure

The constellation mapper operates on the binary bit stream $b(n)$, which is the concatenation of the PLCP preamble, the PLCP header, and the PSDU. $b(n)$ is mapped into one of three constant modulus rotated and differentially encoded constellations: $\frac{\pi}{2}$-DBPSK and $\frac{\pi}{4}$-DQPSK.

The binary bit stream, $b(n)$, for any n in $\{1, \cdots, N\}$, is mapped into the complex sequence a_k, for any k in $\{1, .., N/\log_2(M)\}$ using to the following equation:

$$a_k = a_{k-1} \exp\left(j\phi_k\right), \tag{1}$$

where $a_0 = \exp\left(j\frac{\pi}{2}\right)$, $M = 2, 4, 8$ is the size of the constellation and ϕ_k is the phase change. ϕ_k takes values according to TABLE II for a $\frac{\pi}{2}$-DBPSK mapping and according to TABLE III for a $\frac{\pi}{4}$-DQPSK mapping.

$b(k)$	ϕ_k	$a_k a_{k-1}^*$
0	$\pi/2$	j
1	$3\pi/2$	$-j$

TABLE II: $\frac{\pi}{2}$-DBPSK mapping

$b(2k)$	$b(2k+1)$	ϕ_k	$a_k a_{k-1}^*$
0	0	$\pi/4$	$\exp\left(j\frac{\pi}{4}\right)$
0	1	$3\pi/4$	$\exp\left(j\frac{3\pi}{4}\right)$
1	0	$7\pi/4$	$\exp\left(j\frac{7\pi}{4}\right)$ height1
1	$5\pi/4$	$\exp\left(j\frac{5\pi}{4}\right)$	

TABLE III: $\frac{\pi}{4}$-DQPSK mapping

By choosing a differential mapping, one can get rid of the carrier phase recovery and thus reduce the receiver complexity.

The symbol mapping changes according to the selected frequency band and the data rate. For our simulations, we consider a $\frac{\pi}{2}$-DBPSK constellation mapping for the preamble and the PLCP header and a $\frac{\pi}{4}$-DQPSK modulation for the PSDU. These modulations are specified by the standard for NB-WBAN. As shown in these tables, we note that the product $a_k a_{k-1}^*$ is an imaginary binary modulated signal in the case

[1] $u = (01010101010110110110110 1101)$

of a $\frac{\pi}{2}$-DBPSK mapping and a quaternary modulated signal in the case of a $\frac{\pi}{4}$-DQPSK mapping.

We are going to propose in the next section an adaptive timing recovery algorithm which combines a DA estimator relying on the preamble sequence and a blind estimator for the PLCP header and the PSDU. The time synchronization technique applies to complex gaussian fading channels. The amplitude of the channel fading follows a Rayleigh distribution.

III. Time delay recovery in a non coherent receiver

A. System Model

Let us begin with considering the following transmitted signal $s(t)$:

$$s(t) = \sum_i a_i h(t - iT), \tag{2}$$

where a_i are zero mean i.i.d. transmitted symbols, $h(t)$ is the transmission filter impulse response and T is the symbol period. The received signal is given by:

$$r(t) = \alpha(t)s(t - \tau) + n(t), \tag{3}$$

where τ is an unknown constant time delay introduced by the channel, $\alpha(t)$ is a complex gaussian channel process with a Doppler frequency f_d and $n(t)$ is an additive white Gaussian noise (AWGN) with zero mean and variance σ^2.

Let us consider the N-dimensional truncated vectors $\boldsymbol{r} = [r_1, \cdots, r_N]^T$, $\boldsymbol{s(\tau)} = [s_1(\tau), \cdots, s_N(\tau)]^T$, $\boldsymbol{\alpha} = [\alpha_1, \cdots, \alpha_N]^T$ and $\boldsymbol{n} = [n_1, \cdots, n_N]^T$, representing the N samples of the continuous signals $r(t)$, $s(t - \tau)$ and $n(t)$, respectively. The parameters $\boldsymbol{\alpha}$ and τ and are assumed to be unknown respectively random and deterministic parameters.

Considering that f_d is small compared to the symbol rate $1/T$, then $\alpha(t)$ can be assumed constant over the generic pulse duration. We can write that:

$$r_k = \alpha_k s_k(\tau) + n_k. \tag{4}$$

The matched filtered version of $\boldsymbol{r}$ produces the following signal, after making the time adjustment:

$$x_k(\hat{\tau}) = \alpha_k \sum_i a_i g\left((k-i)T - (\tau - \hat{\tau})\right) + \int_{T_0} h^*(t - kT - \hat{\tau}) n(t) dt. \tag{5}$$

g is the convolution of the transmission filter h with the matched filter and $\hat{\tau}$ is the estimated time delay.

When investigating the timing recovery process, we should differentiate between DA, Decision-Directed (DD) and NDA techniques. The first and the second approaches are motivated by the intuitive notion that timing accuracy can be approved by exploiting the knowledge of the transmitted symbols. Besides, since the transmitted symbols and the channel are jointly estimated by a coherent receiver, a DD and a Channel Aided (ChA) timing recovery technique can be used. A Maximum Likelihood (ML) based Timing Error Detector (TED) can thus be implemented to estimate the time delay. This coherent TED updates the estimated value $\hat{\tau}$ at each signal sample k according to following equation:

$$\hat{\tau}_k = \hat{\tau}_{k-1} + \mu \Re\left\{ \hat{\alpha}_k^* a_k^* \frac{\partial x_k(u)}{\partial u}|_{u=\hat{\tau}_{k-1}} \right\} \tag{6}$$

where μ is the step size, $\hat{\alpha}_k$ is the estimated value of α_k and a_k is replaced by its estimated value $\hat{a}_k$ in a DD context.

However, such algorithm may postpone the receiver start-up [12]. Some limitations may arise with a burst transmission and low latency applications. In that case, it is more secure to rely on NDA methods and non coherent detectors, especially for differentially modulated signals, to avoid channel estimation and carrier phase recovery. Some NDA detectors have already been proposed for AWGN channels such as the Gardner Detector (GD) [4] and the NDA Early Late Detector (NDA-ELD) [13] which use respectively the following updating equations:

$$\hat{\tau}_k = \hat{\tau}_{k-1} + \mu \Re\left\{ x_k(\hat{\tau}_{k-1})^* \left(x_{k+\frac{1}{2}}(\hat{\tau}_{k-1}) - x_{k-\frac{1}{2}}(\hat{\tau}_{k-1}) \right) \right\} \tag{7}$$

and

$$\hat{\tau}_k = \hat{\tau}_{k-1} + \mu \Re\left\{ x_{k-\frac{1}{2}}(\hat{\tau}_{k-1})^* \left(x_{k-1}(\hat{\tau}_{k-1}) - x_k(\hat{\tau}_{k-1}) \right) \right\} \tag{8}$$

It can be shown that the GD and the NDA-ELD are low SNR approximations of the ML TED [12], [14]. So far we have only considered the case of coherent receivers, that use knowledge of the phase of the carrier frequency. In a communications system, there is a phase difference between the reference signal transmitted and the reference signal used in the demodulator. In order to perform a coherent demodulation in the receiver, this phase difference must be estimated and corrected.

The requirement of estimating the carrier phase offset, indeed adds an implementation complexity to the coherent demodulator. For DPSK signals, we usually use a non-coherent demodulator that does not require a carrier phase estimation.

B. Maximum Likelihood Based Non Coherent Timing Error Detector

At the receiver, we usually use a differential decoder for DPSK signals. For that purpose, the demodulated signal is $z_k(u) = x_k(u)x_{k-1}^*(u)$ instead of $x_k(u)$. Considering $d_k = a_k a_{k-1}^*$, the ML non coherent TED estimates the time delay using the following updating equation:

$$\hat{\tau}_k = \hat{\tau}_{k-1} + \beta e_k(d_k, \hat{\tau}_{k-1}), \tag{9}$$

where β is the step size and $e_k(d_k, \hat{\tau}_{k-1})$ is the updating error expressed as:

$$e_k(d_k, \hat{\tau}_{k-1}) = \Re\left\{ d_k^* \frac{\partial z_k(\tau)}{\partial \tau}|_{\tau=\hat{\tau}_{k-1}} \right\}. \tag{10}$$

Such timing error detector is called the Maximum Likelihood Detector (MLD) [12]. In practice, the term $\frac{\partial z_k(\tau)}{\partial \tau}|_{\tau=\tau_{k-1}}$ can be obtained using a polynomial interpolation of the received signal samples and evaluating the derivative of the obtained interpolator at $\hat{\tau}_{k-1}$.

The detector structure is given in Fig.2. The symbols d_k can be known by the receiver only if a_k and a_{k-1} belong to the

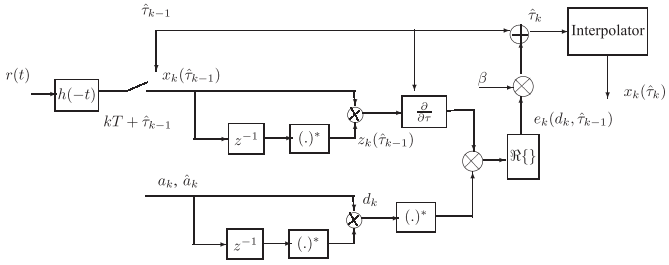

Fig. 2: Non coherent DET structure

preamble. The adaptive algorithm is then called a DA TED. However, if a_k and a_{k-1} belong to the PLCP header or the PSDU, they are unknown by the receiver. In that case, we can implement a DD TED which uses a hard estimate $\hat{d}_k$ instead of d_k. Nevertheless, this alternative leads to higher estimation errors especially at low SNR values for which hard decisions are not reliable.

Although this TED does not require expensive and complex carrier recovery circuits, it is characterized by a poorer bit error rate of detection than the coherent detector.

IV. Simulation Results

In the section, we evaluate the performance of the proposed non coherent TED on a NB-WBAN frame according the standard IEEE 802.15.6. For that purpose, we consider a PPDU composed of 90 $\pi/2-$DBPSK modulated preambule symbols, followed by 31 $\pi/2-$DBPSK modulated PLCP-header symbols and 80 $\pi/4-$DQPSK modulated PSDU symbols. The preambule sequence is known by the receiver, whereas, the PLCP-header and the PSDU are unknown sequences.

The block of 201 symbols is passed through a square root raised cosine transmission filter with a roll-off factor $\alpha = 0.3$. Then the signal is transmitted through Rayleigh channel which introduces a constant time delay τ. At the receiver, the signal is matched filtered.

For the preamble sequence, the timing recovery algorithm operates in the DA mode using equation (9). For the next received data sequence, the synchronizer switches to the DD non coherent TED mode using hard estimates $\hat{d}_k$ of d_k. We have also fixed $f_d T = 0.001$, which means that the channel varies slowly within the observation block.

In Fig. 3 and 4, we plot the MSE curves on the estimation of the normalized time delay, $\hat{\tau}/T$, at each sampling time index using the proposed DD non coherent TED and the NDA coherent TED for a SNR that is respectively equal to 5dB and 10dB. In the NDA coherent approach, τ is estimated using the Gardner detector. These two approaches start at the 91^{th} symbol with the PLCP header.

The black curve serves as a reference and represents the MSE evolution if a DA estimator was implemented. Less MSE is observed at the low SNR value, using the proposed non coherent detector (red curve) in comparison with the coherent detector (green curve) for a $\pi/2-$DBPSK or a $\pi/4-$DQPSK modulation. By increasing the SNR to 10dB, we obtain similar results with both techniques for $\pi/2-$DBPSK modulation and

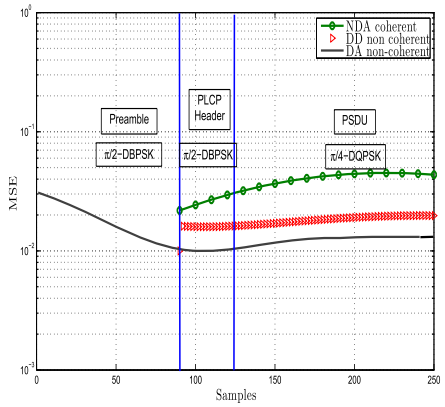

Fig. 3: MSE of the normalized estimated time delay at each sample, SNR=5 dB

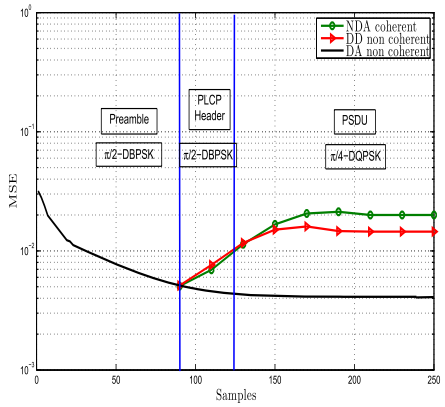

Fig. 4: MSE of the normalized estimated time delay at each sample, SNR=10 dB

we still have an improvement with the proposed detector for a $\pi/4-$DQPSK modulation.

We also note that the MSE increases by using a blind synchronization technique (NDA and DD) instead of a DA TED. It is also increased with the reception of the PSDU, even if a DA TED is chosen, due to the use of a $\pi/4-$DQPSK modulation after the $\pi/2-$DBPSK preamble and PLCP header sequences.

Some numerical results are summarized in the TABLE IV and V for respectively the PLCP header and the PSDU.

TABLE IV: Results at the PLCP Header (100^{th} sample)

Detector	NDA coherent		DD non coherent	
SNR [dB]	5	10	5	10
MSE	2.5×10^{-2}	7×10^{-3}	1.8×10^{-2}	7×10^{-3}

In Fig. 5 and 6, we evaluate the MSE in terms of SNR for respectively $\pi/2-$DBPSK and $\pi/4-$DQPSK modulations and for different Doppler frequency values using a DD non-coherent and NDA coherent detectors. The curves are obtained by averaging the MSE of the different algorithms at the steady

TABLE V: Results at the PSDU (200^{th} sample)

Detector	NDA coherent		DD non coherent	
SNR [dB]	5	10	5	10
MSE	3×10^{-2}	3×10^{-2}	2×10^{-2}	2×10^{-2}

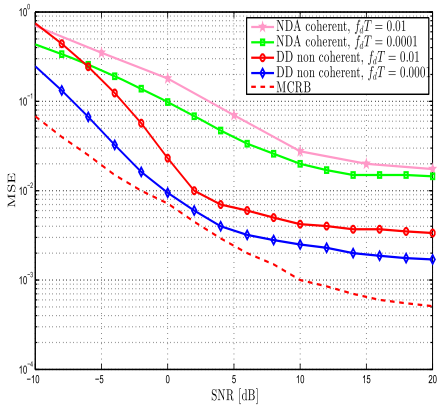

Fig. 5: MSE versus SNR for $\pi/2-$DBPSK mapping

state (after 100 samples) using Monte Carlo simulations. We note that the proposed detector performance is closer to the Modified Cramer Rao Bound (MCRB) [15], which is a theoretical minimum limit of the MSE. The MSE saturation at high SNR is related to the self noise introduced by Inter-Symbol Interference (ISI). Some numerical results are summarized in the TABLE VI for a SNR= 0dB.

TABLE VI: Numerical results for a SNR= 0dB

Detector	Modulation	f_dT	MSE
NDA coherent	$\pi/2-$DBPSK	10^{-4}	0.1
-	-	10^{-2}	0.2
-	$\pi/4-$DQPSK	10^{-4}	0.2
-	-	10^{-2}	0.3
DD non coherent	$\pi/2-$DBPSK	10^{-4}	10^{-2}
-	-	10^{-2}	2×10^{-2}
-	$\pi/4-$DQPSK	10^{-4}	3×10^{-2}
-	-	10^{-2}	4×10^{-2}

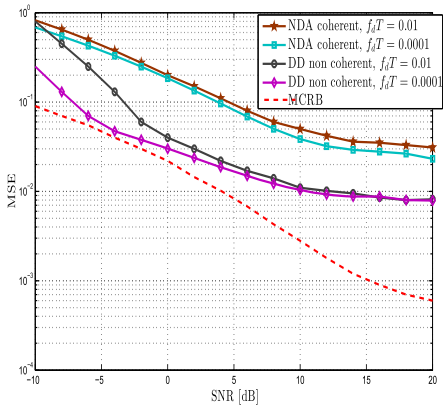

Fig. 6: MSE versus SNR for $\pi/4-$DQPSK mapping

V. Conclusion

To reduce the time synchronizer complexity in a WBAN system under Rayleigh fading channel, we proposed in this paper a DD non coherent timing error detector. This algorithm performs better than a NDA coherent technique, such as the Gardner detector, whose performance are severely degraded at low SNR values. As a future work, the performance of the algorithm can be enhanced by using an adaptive step size [16] or a smoothing off line TED [17]. In order to evaluate such techniques, lower bounds such as those derived in [18] have to be computed.

References

[1] L. Zhou, B. Geller, X. Wang, A. Wei, B. Zheng, and H.-C. Chao, "Multi-User Video Streaming over Multiple Heterogeneous Wireless Networks: A Distributed, Cross-Layer Design Paradigm," *Journal of Internet Technology*, 2009.

[2] "IEEE standard for local and metropolitan area networks - part 15.6: Wireless body area networks," *IEEE Std 802.15.6-2012*, pp. 1–271, Feb. 2012.

[3] K. Mueller and M. Muller, "Timing recovery in digital synchronous data receivers," *IEEE Trans. on Communications*, vol. 24, no. 5, pp. 516–531, 1976.

[4] F. M. Gardner, "A BPSK/QPSK timing-error detector for sampled receivers," *IEEE Trans. on Communications*, vol. 34, no. 5, pp. 423–429, 1986.

[5] C. Berrou, J. Hagenauer, M. Luise, L. Vandendorpe, and C. Schegel, "Turbo-Information processing: algorithms, implementations & applications," *Proc. of the IEEE*, vol. 95, no. 6, pp. 1146 – 1149, Jun. 2007.

[6] I. Nasr, L. Najjar Atallah, B. Geller, and S. Cherif, "CRB derivation and new code-aided timing recovery technique for QAM modulated signals," in *2015 IEEE International Conference on Communications (ICC)*, Jun. 2015, pp. 4901–4906.

[7] I. Nasr, B. Geller, L. Najjar Atallah, and S. Cherif, "Performance study of a near maximum likelihood code-aided timing recovery technique," *IEEE Trans. on Signal Processing*, vol. 64, no. 3, pp. 799–811, Feb 2016.

[8] Diatta, D. D. Geest, and B. Geller, "Reed Solomon turbo codes for high data rate transmission," in *Vehicular Technology Conference, 2004. VTC 2004-Spring. 2004 IEEE 59th*, vol. 2, May 2004, pp. 1023–1027 Vol.2.

[9] I. Nasr, L. Najjar Atallah, S. Cherif, B. Geller, and J. Yang, "A soft maximum likelihood technique for time delay recovery," in *IEEE International Conference on Communications and Networking*, Mar. 2014, pp. 1–5.

[10] I. Nasr, L. Najjar Atallah, S. Cherif, J. Yang, and K. Wang, "On a hybrid preamble/soft-output demapper approach for time synchronization for ieee 802.15.6 narrowband wban," *China Communications*, vol. 12, no. 2, pp. 1–10, Feb 2015.

[11] J. G. Proakis, *Digital Communications*. McGraw-Hill, 1995.

[12] U. Mengali and A. N. D'Andrea, *Synchronization Techniques for Digital Receivers*. Plenum Press, New York and London, 1997.

[13] W. C. Lindsey and M. K. Simon, *Telecommunication Systems Engineering*. Dover Publications, Incorporated, 1991.

[14] M. Oerder, "Derivation of Gardner's timing-error detector from the maximum likelihood principle," *IEEE Trans. on Communications*, vol. 35, no. 6, pp. 684–685, 1987.

[15] A. D'Andrea, U. Mengali, and R. Reggiannini, "The modified Cramer-Rao bound and its application to synchronization problems," *IEEE Trans. on Communications*, vol. 42, no. 234, pp. 1391–1399, Feb. 1994.

[16] J. M. Brossier, P. O. Amblard, and B. Geller, "Self adaptive PLL for general QAM constellations," in *Proc. of 11^{th} European Signal Processing Conference EUSIPCO*, Toulouse, Sept. 2002, pp. 631–635.

[17] J. Yang, B. Geller, C. Herzet, and J. M. Brossier, "Smoothing PLLs for QAM dynamical phase estimation," in *2009 IEEE International Conference on Communications*, June 2009, pp. 1–5.

[18] J. Yang, B. Geller, and A. Wei, "Bayesian and hybrid Cramer-Rao bounds for QAM dynamical phase estimation," in *2009 IEEE International Conference on Acoustics, Speech and Signal Processing*, April 2009, pp. 3297–3300.